

Observation of non-Markovian micro-mechanical Brownian motion

S. Gröblacher,^{1,2} A. Trubarov,² N. Prigge,³ M. Aspelmeyer,^{2,3} and J. Eisert³

¹*Institute for Quantum Information and Matter, California Institute of Technology, Pasadena, CA 91125, USA*

²*University of Vienna, Vienna Center for Quantum Science and Technology (VCQ), Faculty of Physics, A-1090 Vienna, Austria*

³*Dahlem Center for Complex Quantum Systems, Freie Universität Berlin, 14195 Berlin, Germany*

(Dated: July 13, 2022)

At the heart of understanding the emergence of a classical world from quantum theory is the insight that all macroscopic quantum systems are to some extent coupled to an environment and hence are open systems [1–3]. The associated loss of quantum coherence, i.e. decoherence, is also detrimental for quantum information processing applications. In contrast, properly engineered quantum noise can counteract decoherence and can even be used in robust quantum state generation [4–6]. To exploit the detailed dynamics of a quantum system it is therefore crucial to obtain both good knowledge and control over its environment [7, 8]. An explicit modelling of the environment, however, may often not be possible. In this case, simplifying assumptions concerning the nature of the underlying quantum noise are being made that do not necessarily hold for real devices. Micro- and nano-mechanical resonators constitute prominent examples. They are now emerging as promising devices for quantum science [9–14], presently operating in a regime that shares both classical and quantum features. Because of their complex solid-state nature, the properties of their intrinsic surroundings have been the subject of intense research for decades [9]. Here we present a method to reconstruct the relevant properties of the environment, that is, its spectral density, of the center of mass motion of a micro-mechanical oscillator. We observe a clear signature of non-Markovian Brownian motion, which is in contrast to the current paradigm to treat the thermal environment of mechanical quantum resonators as fully Markovian. The presented method, inspired by methods of system identification, can easily be transferred to other harmonic systems that are embedded in a complex environment, for example electronic or nuclear spin states in a solid state matrix [15, 16]. Our results also open up a route for mechanical quantum state engineering via coupling to unorthodox reservoirs.

To understand the role of the environment on a (quantum) mechanical system let us first consider an isolated harmonic oscillator of bare frequency Ω and mass m . In the absence of any coupling its center of mass coordinate q will undergo undamped harmonic motion. In any real physical situation, however, the macroscopic degree of freedom of interest – here the center of mass – will be coupled to some extent to a thermal bath of some temperature. Irrespective of the underlying microscopic mechanism, e.g., phonon scattering in mechanical systems [17] or electronic interactions in superconductors [18], one can usually very well approximate the interaction with the thermal environment as a linear coupling to a bath of harmonic bosonic modes [19]. This is particularly true for high temperatures where finite bath degrees of free-

dom no longer significantly contribute. Such an interaction is described by

$$H_{\text{int}} = q \sum_n c_n q_n \quad (1)$$

where q_n and c_n are the position and coupling strength of the n^{th} bath mode of mass m_n and frequency ω_n , respectively. The dynamics of the system is fully determined by the spectral density of the thermal bath,

$$I(\omega) = \sum_n \frac{c_n^2}{2m_n\omega_n} \delta(\omega - \omega_n), \quad (2)$$

which governs how strongly the oscillator is coupled to specific modes of the environment. This spectral density directly determines the temporal correlations of the thermal driving force. As a consequence, the center of mass experiences a quite drastic change in its motion: it becomes damped, in general in a rather intricate fashion, and is shifted in its frequency. This *quantum Brownian motion* [20, 21] is one of the most paradigmatic models of decoherence in quantum theory [1, 2].

All current theoretical studies on micro- and nano-mechanical quantum systems make the explicit or implicit assumption that the decohering quantum dynamics is Markovian: This means that the open systems dynamics is forgetful [22–24]. In this case the two-point correlation function of the thermal force equals $k_B T \delta(t - t')$ and is hence uncorrelated in time. For a weakly damped mode at high temperatures (and in contrast to the situation in spin-Bose models [25]), such Markovian quantum dynamics is found for an *Ohmic spectral density*

$$I(\omega) \propto \omega \quad (3)$$

over large frequency ranges. For such damped harmonic systems in the high temperature limit, spectral densities other than Ohmic ones lead to deviations from Markovian evolutions.

In many solid-state systems this approximation has been found to be both theoretically plausible and experimentally valid to extraordinarily high precision [3]. Various loss mechanisms in mechanical resonators, however, are known to exhibit a strong frequency dependence [7, 8, 17, 26, 27], which challenges the general validity of the Markov approximation even for simple mechanical quantum devices. We introduce a straight-forward test to directly characterize the spectral properties of the environment in the vicinity of the mechanical mode. Because of the complex solid-state architecture of these resonators computing the spectral density from first

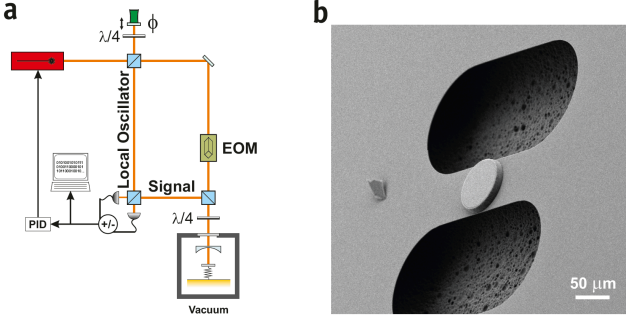


FIG. 1. **Sketch of the experiment.** **a** The experimental setup consist of a 1064 nm Nd:YAG laser, which is split into a signal beam and a local oscillator (LO). The signal is phase modulated with an electro-optical modulator (EOM) for Pound-Drever-Hall locking of the opto-mechanical cavity. In order to read-out the phase of the signal beam acquired from the motion of the mechanical resonator, it is beaten with a strong local oscillator (LO) on a beamsplitter and detected on two photodiodes. The phase ϕ between the LO and the signal is stabilised with the help of a mirror mounted on a piezo-ceramic actuator in order to only detect the phase quadrature of the signal field. The opto-mechanical cavity is kept at a pressure of $< 10^{-3}$ mbar to avoid residual-gas damping of the mechanical motion. **b** Scanning electron microscope picture of the tested device.

principles seems a tedious if not impossible task, with the exception of well isolated mechanisms. Instead of making a priori assumptions about the dynamics, our approach is rather in the spirit of *open system identification*: we measure the properties that give rise to a quantitative estimate on the Markovian nature of the dynamics.

Our approach relies on monitoring the mechanical motion with high sensitivity. We achieve this by weakly coupling the mechanics to an optical cavity field whose phase response encodes the mechanical motion. We then make use of the fact that the shape of the bath spectral density affects the amplitude response of the mechanical resonator upon thermal driving. Specifically, the experimentally accessible spectrum of the cavity output light for high temperatures is given by

$$S_{\delta Y^{\text{out}}}(\omega) \approx c \frac{I(\omega)}{\omega ((\Omega_{\infty}^2 - \omega^2)^2 + (\gamma_{\infty} \omega)^2)}, \quad (4)$$

for a suitable constant $c > 0$ (for details, see the supplementary material). Here, δY^{out} is the optical phase quadrature, which can be made a direct measure of the mechanical position quadrature q and which is obtained by optical homodyne readout, Ω_{∞} is the renormalised mechanical frequency, and γ_{∞} is the effective asymptotic mechanical damping constant. The opto-mechanical device can hence be seen as an ultra-sensitive *black box* measuring the spectral density.

We demonstrate our analysis on a micromechanical resonator as shown in Figure 1b. The device consists of a 1 μm thick layer of Si_3N_4 and is 150 μm long and 50 μm wide. The 50 μm diameter, high-reflectivity ($R > 99.991\%$) mirror pad in its center allows to use this resonator as a mechanically moving end mirror in a Fabry-Pérot cavity, as has been done to explore the regime of cavity opto-mechanical

coupling [28, 29] (for details on the fabrication process see Ref. [30]). In our case, the cavity finesse is intentionally kept low at $F = 2300$ by choosing a high-transmittivity input mirror. This results in an amplitude cavity decay rate of $\kappa = 1.3$ MHz (cavity length: 25 mm). By using a signal beam of 100 μW , we realize a sufficiently weak opto-mechanical coupling $g = G_0|\alpha_s| \approx 40$ kHz $\ll \kappa$, such that the cavity field phase quadrature adiabatically follows the mechanical motion and hence δY^{out} is a reliable measure of q . The fundamental mechanical resonance frequency is $\Omega = 2\pi \times 914$ kHz, with a mechanical quality Q -factor of approximately 215 at room temperature. Optical homodyne detection of the outgoing cavity field finally yields the temporal phase quadrature fluctuations $\delta Y^{\text{out}}(t)$, which are digitized to calculate the noise power spectrum $S_{\delta Y^{\text{out}}}(\omega)$ (see Fig. 1a). All experiments have been performed in vacuum (background pressure $< 10^{-3}$ mbar) to prevent the influence of viscous gas damping. At the mentioned parameters for our experiment we achieve a displacement sensitivity of approx. $3 \times 10^{-15} \text{m}/\sqrt{\text{Hz}}$ as is shown in Fig. 2. To exclude the possible influence of spurious background noise we have also characterized the noise power spectrum of the cavity field without a mechanical resonator. In our configuration this is possible due to the specific design of the chip comprising the micromechanical device, which holds several non-suspended mirror pads which can be used by slightly moving the chip. The resulting noise power spectrum is flat and hence cavity noise cannot contribute to any non-Brownian spectral signal (see Fig. 2). Another possible spectral dependence could arise from the presence of higher-order mechanical modes, which are not taken into account in Eq. (4). A finite element analysis of our mechanical system reveals the next mechanical mode at $\Omega^{(1)} = 2\pi \times 1.2$ MHz. As can be seen from Fig. 2, the spectral overlap in the vicinity of Ω is many orders of magnitude below the measured signal and hence negligible.

After characterizing the resonator the final task to perform bath spectroscopy now reduces to assessing the statistical significance of a single assumption: namely that the spectral density is locally, i.e. in the vicinity of Ω , well described by

$$I(\omega) = C\omega^k, \quad (5)$$

for some $C > 0$ and $k \in \mathbb{R}$. A value of $k = 1$ corresponds to an *Ohmic environment*, $k > 1$ to a *supra-Ohmic*, and $k < 1$ to a *sub-Ohmic* environment. This is the common classification of spectral densities [21]. For a slowly varying spectral density, however, what largely determines the stationary state is the slope of the spectral density in the vicinity of Ω .

The starting point of this analysis is Eq. (4). From the homodyning measurement, samples of statistically independent subsets of time series are formed, and data sets are obtained as Fourier transforms thereof. For each of these independently distributed Fourier transforms, one identifies the optimal k in Eq. (4) with $I(\omega) = C\omega^k$ that minimises the least square deviation, within a suitable frequency interval $[\omega_{\min}, \omega_{\max}]$. Here $\omega_{\min} = 885$ kHz and $\omega_{\max} = 945$ kHz are chosen, but the results are largely independent of that choice. Interestingly, it is the comparably bad mechanical Q -factor that allows for the assessment of a relatively large frequency interval. For each

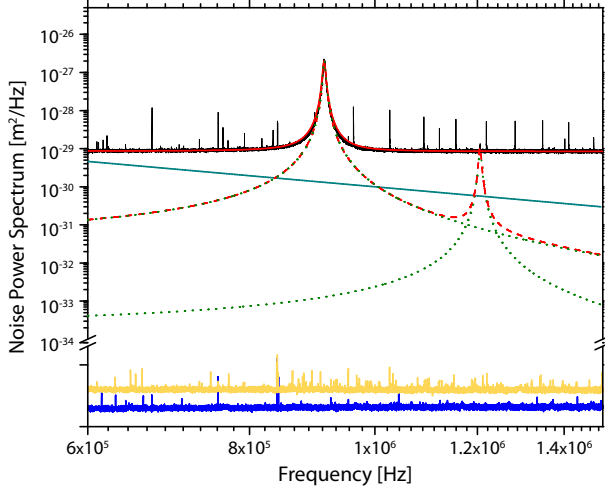


FIG. 2. **Noise power spectra.** Depicted are the spectra obtained with the mechanics being part of the setup (black) (with a fit in red), with no mechanics (yellow), with no cavity (blue), a spectrum reflecting a sub-Ohmic spectral density $I(\omega) \propto \omega^{-2}$ (turquoise), the simulated sum (red dashed) and the simulated modes (green dotted). In our simulation we have assumed the mechanical Qs of the higher order modes to be similar to the fundamental mode, which is in good agreement with typical experimental values. Note that for clarity the measurements of the additional noise (yellow and blue) are not to scale.

individual data set, several different values of the power k are compatible with the data, which is an unsurprising finding in the light of the presence of noise in the data. Given the large data set that is available, however, one can arrive at an estimate of the optimal coefficient k with large statistical significance.

The main result is shown in Fig. 3. The histogram over all optimal power estimates yields $k = -2.30 \pm 1.05$, which is a clear deviation from $k = 1$ for an Ohmic bath density. In other words, our analysis shows that the heat bath of the micromechanical oscillator is not consistent with Markovian damping of a quantum harmonic oscillator in the high temperature limit. While we do not expect effects of finite-dimensional bath components resulting, e.g., from two-level fluctuators, to measurably influence the result [31–33], we cannot rigorously exclude such contributions. We can yet strictly and unambiguously falsify the common assumption of a harmonic Ohmic heat bath. Our specific situation is rather described by highly sub-Ohmic damping. It is known that in non-Ohmic baths the coefficients of the master equation governing the dynamics are becoming strongly time-dependent [21]. This means that while the steady-state properties of a mechanical system may be modified only in a mild way – the deviations of the measured spectrum from Eq. (4) for Ohmic spectral densities are small – one should expect larger deviations for predictions in time-dependent situations [34]. It has been pointed out recently that such non-Markovian quantum noise can significantly influence the ability to generate quantum entanglement [35]. Indeed, intricate memory effects come into play in case of non-Markovian dynamics, giving rise to a picture of decoherence beyond basic rate equations.

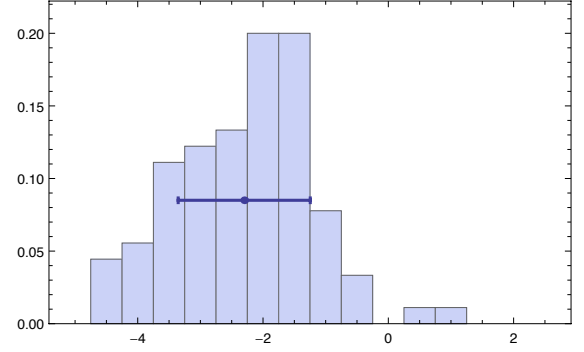


FIG. 3. **Estimated coefficients.** Depicted is the histogram of best estimated coefficients k in the local approximation of the spectral density by $I(\omega) = C\omega^k$, showing a statistically significant deviation from the Ohmic situation of $k = 1$.

Finally, our findings complement related research in mechanical engineering. It is known that damping due to internal materials losses can be different from a purely velocity dependent damping of a simple harmonic oscillator and can give rise to a modified thermal noise power spectral density [36, 37]. Specific models for such non-viscous damping, in particular for thermoelastic damping, have been extensively studied in the context of both gravitational wave detection [26, 27, 36] and measurements of the gravitational constant [38, 39], where thermal noise in the tail of a mechanical resonance poses limits on the achievable sensitivity. In turn, while the accurate measurement of internal friction and the analysis of their origin remains a challenging task, broadband thermal noise measurements have become an important input for the design and engineering of high-Q micro- and nanomechanical resonators [40]. Our approach adds two new aspects: First, our analysis provides direct access to ‘Markovianity’ [22–24] as a statistical property of the environment of a quantum harmonical oscillator. Second, we exploit the enhancement of the thermal noise in the vicinity of the mechanical resonance, instead of probing thermal noise over a broad frequency band. This provides a local estimate of the thermal bath characteristics, which is the relevant property for non-Brownian dynamics (see supplementary material). In a next step, combining this method with a sweep in resonance frequency [41] could provide direct, full broadband mechanical spectroscopy of the thermal bath spectral density, in a ‘tomographic approach’. Our system identification approach is also model-independent, i.e., we do not make any prior assumptions on the underlying nature of the dissipation or on the specific shape of the thermal noise spectral density (other than assuming harmonicity). Although the current study is performed at room temperature, in the ‘classical’ regime, it can be directly applied to other mechanical resonators that operate close to the quantum regime [10, 11, 42].

In summary, we have introduced a versatile method to directly probe the spectral density of the heat bath of a micromechanical resonator. We demonstrate that the common assumption of Markovian Brownian motion does not hold. This opens the way towards systematic studies of individual dissipation

channels such as two-level fluctuators [31, 32]. In combination with the possibility to geometrically modify the phonon spectrum [17, 43, 44] this would allow for full reservoir engineering of quantum harmonic oscillators. We hope that the present work stimulates such further experimental analysis of unorthodox decoherence phenomena opening up alongside technological development.

We acknowledge discussions with I. Wilson-Rae, J.-P. Paz,

B.-L. Hu, C. Fleming, D. Loss, G. Milburn, P. Rabl, G. Cole and A. Mari, and contributions to the statistical estimation by K. Kieling. This work has been supported by the EU (QESSENCE, MINOS, ITN cQOM, RAQUEL and a Marie Curie fellowship of S. G.), the EURYI, the ERC (StG of M. A. and J. E.), the BMBF (QuOREP), the Austrian Science Fund FWF (START, FOQUS), and the Alexander von Humboldt Foundation (Bessel Research Award of M. A.).

-
- [1] Joos, E. *et al.* *Decoherence and the appearance of a classical world in quantum theory* (Springer, Heidelberg, 1996).
 - [2] Zurek, W. H. Decoherence, einselection, and the quantum origins of the classical. *Rev. Mod. Phys.* **75**, 715–775 (2003).
 - [3] Gardiner, C. W. & Zoller, P. *Quantum noise* (Springer Series in Synergetics, 2004).
 - [4] Verstraete, F., Wolf, M. M. & Cirac, J. I. Quantum computation and quantum-state engineering driven by dissipation. *Nature Phys.* **5**, 633–636 (2009).
 - [5] Diehl, S. *et al.* Quantum states and phases in driven open quantum systems with cold atoms. *Nature Phys.* **4**, 878–883 (2008).
 - [6] Kastoryano, M. J., Wolf, M. M. & Eisert, J. Precisely timing dissipative quantum information processing. *Phys. Rev. Lett.* **110**, 110501 (2013).
 - [7] Koppens, F. H. L. *et al.* Universal phase shift and non-exponential decay of driven single-spin oscillations. *Phys. Rev. Lett.* **99**, 106803 (2007).
 - [8] Medford, J. *et al.* Scaling of dynamical decoupling for spin qubits. *Phys. Rev. Lett.* **108**, 086802 (2012).
 - [9] Knobel, R. G. & Cleland, A. N. Nanometre-scale displacement sensing using a single electron transistor. *Nature* **424**, 291–293 (2003).
 - [10] O’Connell, A. D. *et al.* Quantum ground state and single-phonon control of a mechanical resonator. *Nature* **464**, 697–703 (2010).
 - [11] Safavi-Naeini, A. H. *et al.* Observation of quantum motion of a nanomechanical resonator. *Phys. Rev. Lett.* **108**, 033602 (2012).
 - [12] Chan, J. *et al.* Laser cooling of a nanomechanical oscillator into its quantum ground state. *Nature* **478**, 89–92 (2011).
 - [13] Stannigel, K. *et al.* Single-photon nonlinearities in two-mode optomechanics. *Phys. Rev. Lett.* **109**, 013603 (2012).
 - [14] Aspelmeyer, M., Gröblacher, S., Hammerer, K. & Kiesel, N. Quantum optomechanics – throwing a glance. *J. Opt. Soc. Am. B* **27**, A189–A197 (2010).
 - [15] Hanson, R., Kouwenhoven, L. P., Petta, J. R., Tarucha, S. & Vandersypen, L. M. K. Spins in few-electron quantum dots. *Rev. Mod. Phys.* **79**, 1217–1265 (2007).
 - [16] Weber, J. R. *et al.* Quantum computing with defects. *PNAS* **107**, 8513–8518 (2010).
 - [17] Wilson-Rae, I. Intrinsic dissipation in nanomechanical resonators due to phonon tunneling. *Phys. Rev. B* **77**, 245418 (2008).
 - [18] Leggett, A. J. Quantum tunneling in the presence of an arbitrary linear dissipation mechanism. *Phys. Rev. B* **30**, 1208–1218 (1984).
 - [19] Feynman, R. P. & Vernon, F. L. The theory of a general quantum system interacting with a linear dissipative system. *Ann. Phys.* **24**, 118–173 (1963).
 - [20] Caldeira, A. O. & Leggett, A. J. Path integral approach to quantum brownian motion. *Physica A* **121**, 587–616 (1983).
 - [21] Hu, B. L., Paz, J. P. & Zhang, Y. Quantum brownian motion in a general environment: Exact master equation with nonlocal dissipation and colored noise. *Phys. Rev. D* **45**, 2843–2861 (1992).
 - [22] Wolf, M. M., Eisert, J., Cubitt, T. S. & Cirac, J. I. Assessing non-markovian dynamics. *Phys. Rev. Lett.* **101**, 150402 (2008).
 - [23] Rivas, A., Huelga, S. F. & Plenio, M. B. Entanglement and non-markovianity of quantum evolutions. *Phys. Rev. Lett.* **105**, 050403 (2010).
 - [24] Laine, E.-M., Piilo, J. & Breuer, H.-P. Measure for the non-markovianity of quantum processes. *Phys. Rev. A* **81**, 062115 (2010).
 - [25] DiVincenzo, D. P. & Loss, D. Rigorous born approximation and beyond for the spin-boson model. *Phys. Rev. B* **71**, 035318 (2005).
 - [26] González, G. I. & Saulson, P. R. Brownian motion of a torsion pendulum with internal friction. *Phys. Lett. A* **201**, 12–18 (1995).
 - [27] Kajima, M., Kusumi, N., Moriwaki, S. & Mio, N. Wide-band measurement of mechanical thermal noise using a laser interferometer. *Phys. Lett. A* **263**, 21–26 (1999).
 - [28] Gröblacher, S. *et al.* Demonstration of an ultracold micro-optomechanical oscillator in a cryogenic cavity. *Nature Phys.* **5**, 485–488 (2009).
 - [29] Gröblacher, S., Hammerer, K., Vanner, M. R. & Aspelmeyer, M. Observation of strong coupling between a micromechanical resonator and an optical cavity field. *Nature* **460**, 724–727 (2009).
 - [30] Gröblacher, S. *Quantum opto-mechanics with micromirrors: combining nano-mechanics with quantum optics*. Ph.D. thesis, Universität Wien (2010).
 - [31] Verhagen, E., Deléglise, S., Weis, S., Schliesser, A. & Kippenberg, T. J. Quantum-coherent coupling of a mechanical oscillator to an optical cavity mode. *Nature* **482**, 63–67 (2012).
 - [32] Lisenfeld, J. *et al.* Rabi spectroscopy of a strongly driven qubit-fluctuator system. *Phys. Rev. B* **81**, 100511 (2010).
 - [33] Schlosshauer, M., Hines, A. P. & Milburn, G. J. Decoherence and dissipation of a quantum harmonic oscillator coupled to two-level systems. *Phys. Rev. A* **77**, 022111 (2008).
 - [34] Mari, A. & Eisert, J. Gently modulating optomechanical systems. *Phys. Rev. Lett.* **103**, 213603 (2009).
 - [35] Ludwig, M., Hammerer, K. & Marquardt, F. Entanglement of mechanical oscillators coupled to a non-equilibrium environment. *Phys. Rev. A* **82**, 012333 (2010).
 - [36] Saulson, P. Thermal noise in mechanical experiments. *Phys. Rev. D* **42**, 2437–2445 (1990).
 - [37] Prabhakar, S. & Vengallatore, S. Theory of thermoelastic damping in micromechanical resonators with two-dimensional heat conduction. *J. Microelectromech. S.* **17**, 494–502 (2008).
 - [38] Bernardini, A. *et al.* Characterization of mechanical dissipation spectral behavior using a gravitomagnetic pendulum. *Phys. Lett. A* **255**, 142–146 (1999).

- [39] Yang, S.-Q. *et al.* Direct measurement of the anelasticity of a tungsten fiber. *Phys. Rev. D* **80**, 1–12 (2009).
- [40] Sosale, G., Almecija, D., Das, K. & Vengallatore, S. Mechanical spectroscopy of nanocrystalline aluminum films: effects of frequency and grain size on internal friction. *Nanotechnology* **23**, 155701 (2012).
- [41] Jöckel, A. *et al.* Spectroscopy of mechanical dissipation in micro-mechanical membranes. *Appl. Phys. Lett.* **99**, 143109 (2011).
- [42] Teufel, J. D. *et al.* Sideband cooling of micromechanical motion to the quantum ground state. *Nature* **475**, 359–363 (2011).
- [43] Anetsberger, G., Rivière, R., Schliesser, A., Arcizet, O. & Kippenberg, T. J. Ultralow-dissipation optomechanical resonators on a chip. *Nature Photon.* **2**, 627–633 (2008).
- [44] Cole, G. D., Wilson-Rae, I., Werbach, K., Vanner, M. R. & Aspelmeyer, M. Phonon-tunneling dissipation in mechanical resonators. *Nature Comm.* **2**, 231 (2011).
- [45] Genes, C., Vitali, D., Tombesi, P., Gigan, S. & Aspelmeyer, M. Ground-state cooling of a micromechanical oscillator: generalized framework for cold damping and cavity-assisted cooling schemes. *Phys. Rev. A* **77**, 033804 (2008).

I. SUPPLEMENTARY MATERIAL

A. Noise-noise correlations for the damped mode

We start from the Hamiltonian of the Caldeira-Leggett-model (or Ullersma model) for quantum Brownian motion [20, 21], so the standard quantum mechanical damped oscillator,

$$H_m = \frac{p^2}{2m} + \frac{1}{2}m\Omega^2 q^2 + \sum_n \left(\frac{p_n^2}{2m_n} + \frac{1}{2}m_n\omega_n^2 q_n^2 \right) + q \sum_n c_n q_n. \quad (6)$$

At this point no assumption is made with respect to the coupling except from it being linear. The equations of motion of the canonical coordinate of the oscillator as such are given by

$$\ddot{q}(t) + \Omega^2 q(t) + \frac{2}{m} \int_0^t ds \eta(t-s) q(s) = \frac{f(t)}{m}. \quad (7)$$

Here, the inhomogeneity is given by

$$f(t) = - \sum_n c_n \left(q_n(0) \cos(\omega_n t) + \frac{p_n(0)}{m_n} \frac{\sin(\omega_n t)}{\omega_n} \right), \quad (8)$$

whereas the damping kernel η is

$$\eta(s) = \frac{d}{ds} \nu(s), \quad (9)$$

$$\nu(s) = \int_0^\infty d\omega \frac{I(\omega)}{\omega} \cos(\omega s), \quad (10)$$

in terms of the spectral density

$$I(\omega) = \sum_n \delta(\omega - \omega_n) \frac{c_n^2}{2m_n\omega_n}. \quad (11)$$

In the Ohmic regime, so for a spectral density linear in ω until a finite cut-off frequency Λ , this damping kernel is for large Λ arbitrarily well approximated by an expression of the form

$$\eta(t) = \gamma_\infty m \delta'(t), \quad (12)$$

so Eq. (7) takes a form local in time. Returning to the general case, the exact two-point correlation functions of the thermal force are found to be

$$\langle f(t)f(s) \rangle = \int_{-\infty}^\infty e^{i\omega(t-s)} \frac{\hbar}{2} I(\omega) \times \left(\coth \left(\frac{\hbar\omega}{2k_B T} \right) - 1 \right) d\omega, \quad (13)$$

for $t, s \geq 0$, where for simplicity of notation we have extended the definition of the spectral density to $I : \mathbb{R} \rightarrow \mathbb{R}$ by taking $I(-\omega) = -I(\omega)$.

This expression, valid in general without any approximation, can be cast into a time-local form, albeit the dynamics being non-Markovian. For this, one has to formulate the Green's function $G : \mathbb{R} \rightarrow \mathbb{R}$ of the problem. One arrives at a differential equation of the form

$$\ddot{q}(t) + \Omega^2(t)q(t) + \gamma(t)\dot{q}(t) = \frac{\bar{f}(t)}{m} \quad (14)$$

for $t \geq 0$, where now the time-dependent damping is found to be

$$\gamma(t) = \frac{G(t)\ddot{G}(t) - \dot{G}(t)\dot{G}(t)}{\dot{G}(t)^2 - G(t)\ddot{G}(t)}, \quad (15)$$

and

$$\Omega^2(t) = \frac{\ddot{G}(t)^2 - \dot{G}(t)\ddot{G}(t)}{\dot{G}(t)^2 - G(t)\ddot{G}(t)}. \quad (16)$$

The inhomogeneity becomes

$$\bar{f}(t) = (\partial_t^2 + \gamma(t)\partial_t + \Omega(t)^2) \int_0^t G(t-s)f(s)ds. \quad (17)$$

It can now be shown, and is physically plausible, that these quantities take their asymptotic values for large times,

$$\lim_{t \rightarrow \infty} \gamma(t) = \gamma_\infty, \quad \lim_{t \rightarrow \infty} \Omega(t) = \Omega_\infty. \quad (18)$$

These expressions are exact and no approximations have been made until this point. For large times t , the expression

$$\ddot{q}(t) + \Omega_\infty^2 q(t) + \gamma_\infty \dot{q}(t) \quad (19)$$

is arbitrarily well approximated by $\bar{f}(t)/m$. In fact, the correlation function of this modified driving can readily be found by going into the Fourier domain, with convention taken

$$\tilde{F}(\omega) = \int_{-\infty}^\infty F(t)e^{-i\omega t} dt. \quad (20)$$

An evaluation of this expression reveals that the Fourier transform of the Green's function is given by

$$\tilde{G}(\omega) = \frac{1}{-\omega^2 + 2i\hat{\eta}(\omega)/m + \Omega_\infty^2}, \quad (21)$$

where we have defined $\hat{\eta}$ and analogously $\hat{\nu}$ as

$$\hat{\eta}(\omega) = \int_0^\infty dt \eta(t)e^{-i\omega t}. \quad (22)$$

The expected two-time correlation function of \bar{f} is then computed to be

$$\begin{aligned} \langle \bar{f}(t)\bar{f}(s) \rangle &= \int_{-\infty}^\infty e^{i\omega(t-s)} \frac{\hbar}{2} I(\omega) \left(\coth \left(\frac{\hbar\omega}{2k_B T} \right) - 1 \right) \\ &\times ((\Omega_\infty^2 - \omega^2)^2 + \gamma_\infty \omega^2) |\tilde{G}(\omega)|^2 d\omega \\ &= \int_{-\infty}^\infty e^{i\omega(t-s)} \frac{\hbar}{2} I(\omega) \\ &\times \frac{(\Omega_\infty^2 - \omega^2)^2 + \gamma_\infty \omega^2}{(\Omega^2 - \omega^2 + 2\text{Re}(\hat{\eta}(\omega))/m)^2 + (2\text{Im}(\hat{\eta}(\omega))/m)^2} \\ &\times \left(\coth \left(\frac{\hbar\omega}{2k_B T} \right) - 1 \right) d\omega, \end{aligned} \quad (24)$$

for $t, s \geq 0$. We also find in terms of ν , rather than in η ,

$$\langle \bar{f}(t)\bar{f}(s) \rangle = \int_{-\infty}^{\infty} \frac{(\Omega_{\infty}^2 - \omega^2)^2 + \gamma_{\infty}^2 \omega^2}{(K^2 - \omega^2 + 2\omega \text{im}(\hat{\nu}(\omega))/m)^2 + (2\omega \text{re}(\hat{\nu}(\omega))/m)^2} \times \frac{\hbar}{2} I(\omega) \left(\coth\left(\frac{\hbar\omega\beta}{2}\right) - 1 \right) e^{i\omega(t-s)} d\omega, \quad (25)$$

where

$$K^2 = -\frac{2}{m}\nu(0) + \Omega^2. \quad (26)$$

This is still an exact expression. The real part is now identified to be

$$\text{re}(\hat{\nu}(\omega)) = \frac{\pi I(\omega)}{2\omega}. \quad (27)$$

The weak coupling approximation amounts to approximating

$$\Omega_{\infty}^2 \approx K^2, \quad \gamma_{\infty} \approx \frac{\pi I(K)}{mK}, \quad (28)$$

which is true if

$$\left| \frac{2}{m} \partial_{\omega} \hat{\nu}(\omega) |_{\omega=K} \right| \ll 1, \quad (29)$$

$$\left| \frac{1}{m} \hat{\nu}(K) \right| \ll K \quad (30)$$

and if the imaginary part is negligible. This is the standard weak coupling limit, which is the only approximation made in the discussion of quantum Brownian motion. Note that this weak coupling limit does not require the coupling to be so weak for the rotating wave approximation or the ‘quantum optical limit’ (see Subsection I C) to be valid. With these approximations, one finds that

$$\frac{(\Omega_{\infty}^2 - \omega^2)^2 + \gamma_{\infty}^2 \omega^2}{(K^2 - \omega^2 + \omega \frac{2}{M} \text{im}(\hat{\nu}(\omega)))^2 + (\omega \frac{2}{M} \text{re}(\hat{\nu}(\omega)))^2} \quad (31)$$

is extraordinarily well approximated by unity, meaning that the contribution of the spectral density to the two-time correlation function of \bar{f} originates only from the nominator. This is basically the reason, why in Eq. (25) $I(\omega)$ appears only in the numerator. Within this approximation, we have that $\langle \bar{f}(t)^2 \rangle \approx \langle f(t)^2 \rangle$ to a very good approximation.

B. Relating the spectra of the mirror and the output light

We now discuss the situation where the harmonic oscillator described above is coupled to a laser field within an optical cavity. The vibrational mode of a high reflective micro-mirror is modeled as a damped harmonic oscillator as in Eq. (6). The micro-mirror together with another solid mirror forms an optical cavity, which is driven by a laser beam. The total Hamiltonian of a harmonic oscillator coupled to thermal bath and laser field within a driven optical cavity is given by

$$H = H_m + \hbar\omega_c a^\dagger a - \hbar g_0 a^\dagger a q + i\hbar E (a^\dagger e^{-i\omega_0 t} - a e^{i\omega_0 t}), \quad (32)$$

where a is the annihilation operator of the optical mode, $g_0 = \omega_c/L$ is the coupling constant of the mechanical to the optical mode. ω_c is the resonance frequency of the cavity with length L and decay rate κ . H_m is the complete Hamiltonian of the distinguished mechanical mode with its environment as in Eq. (6).

$$|E| = \sqrt{2W\kappa/(\hbar\Omega)}, \quad (33)$$

where W is the input power of the laser with frequency ω_0 . The Heisenberg picture equations of motion formulated in the interaction picture with respect to $\hbar\omega_0 a^\dagger a$ become, suppressing time dependence,

$$\dot{q} = \frac{p}{m}, \quad (34)$$

$$\dot{p} = -m\Omega^2 q - \sum_n c_n q_n + \hbar g_0 a^\dagger a, \quad (35)$$

$$\dot{a} = -(\kappa + i\Delta_0)a + ig_0 a q + E + \sqrt{2\kappa} a^{\text{in}}, \quad (36)$$

$$\dot{q}_n = \frac{p_n}{m_n}, \quad (37)$$

$$\dot{p}_n = -m_n \omega_n^2 q_n - c_n q, \quad (38)$$

where $\Delta_0 = \omega_c - \omega_0$. In the weak-coupling limit of the previous subsection, the equations of motion turn into

$$\ddot{q} + \gamma_{\infty} \dot{q} + \Omega_{\infty}^2 q = \frac{\bar{f}}{m} + \frac{\hbar g_0}{m} a^\dagger a, \quad (39)$$

$$\dot{a} = -(\kappa + i\Delta_0)a + ig_0 a q + E + \sqrt{2\kappa} a^{\text{in}}, \quad (40)$$

again suppressing time dependence. Based on these expressions, one can proceed exactly as presented in Ref. [45], with the Ohmic bath being replaced by this general thermal bath. In order to progress, it is helpful to make use of dimensionless quantities,

$$Q = \frac{q}{l}, \quad P = \frac{pl}{\hbar}, \quad l = \sqrt{\hbar/(m\Omega_{\infty})} \quad (41)$$

and to define $G_0 = g_0 l$. Following Ref. [45], one arrives at an expression which is for large times t, s well approximated by

$$\langle \delta Q(t) \delta Q(s) \rangle \approx \int_{-\infty}^{\infty} \frac{d\omega}{2\pi} |\chi_{\text{eff}}^{\Delta}(\omega)|^2 (S_{\text{th}}(\omega) + S_{\text{rp}}(\omega, \Delta)) e^{i\omega(t-s)}, \quad (42)$$

for the deviations from the asymptotic steady state value

$$\delta Q = Q - \lim_{t \rightarrow \infty} \langle Q \rangle = Q - \frac{G_0 |\alpha_s|^2}{\Omega_{\infty}}, \quad (43)$$

where

$$S_{\text{th}}(\omega) = \frac{\pi I(\omega)}{m\Omega_{\infty}} \left(\coth\left(\frac{\hbar\omega}{2k_B T}\right) - 1 \right), \quad (44)$$

$$S_{\text{rp}}(\omega, \Delta) = \frac{2\kappa G_0^2 |\alpha_s|^2}{\Delta^2 + \kappa^2 + \omega^2 + 2\Delta\omega}, \quad (45)$$

$$\chi_{\text{eff}}^{\Delta}(\omega) = \Omega_{\infty} \left(\Omega_{\infty}^2 + i\gamma_{\infty}\omega - \omega^2 - \frac{2G_0^2 |\alpha_s|^2 \Delta \Omega_{\infty}}{\Delta^2 + (\kappa + i\omega)^2} \right)^{-1} \quad (46)$$

Here, Δ and α_s are implicitly defined as

$$\Delta = \Delta_0 - \frac{G_0^2 |\alpha_s|^2}{\Omega_{\infty}}, \quad \alpha_s = \lim_{t \rightarrow \infty} \langle a \rangle = \frac{E}{\kappa + i\Delta}. \quad (47)$$

This is different from the expression in Ref. [45] in that both the thermal noise spectrum S_{th} as well as the radiation pressure noise spectrum S_{rp} are being altered.

The final step is to include the actual measurement of the opto-mechanical system and how the information about the motion of the mechanics can be obtained from the measurement of the light leaking out of the cavity. As before, this entire apparatus is assumed to be well-characterized and known, which is a very reasonable assumption for the present experiment.

In the experiment the light leaking out of the optical cavity, referred to as ‘signal’, is measured by homodyne detection. This means that signal is mixed on a 50:50 beam-splitter with a second, much stronger laser beam. This second beam has the same frequency as the light driving the cavity and is referred to as the ‘local oscillator’. The intensities measured in both arms are then electronically subtracted. The result is a voltage, which apart from delta-correlated measurement noise is proportional to some general quadrature of the signal, depending on the phase between the signal and the local oscillator and is, apart from noise, proportional to the corresponding intra-cavity quadrature. In the parameter regime relevant here, it turns out that the output quadrature δY^{out} is proportional to δQ subjected to additional noise. Hence, by measuring this quadrature of the signal, information about the mechanical motion and therefore about the thermal bath driving the mechanics can be extracted.

Again following Ref. [45], one arrives in the regime that is experimentally relevant at the expression for the spectrum of the output light measured with quantum efficiency $\zeta > 0$ that is very well approximated by the expression in dimensionless units

$$S_{\delta Y^{\text{out}}}(\omega) \approx \frac{8k_B T \pi \zeta G_0^2 |\alpha_s|^2 \Omega_{\infty}}{m\hbar\kappa} \frac{I(\omega)}{\omega ((\Omega_{\infty}^2 - \omega^2)^2 + (\gamma_{\infty}\omega)^2)}. \quad (48)$$

That is to say, by detecting the output light, one can immediately obtain information on the spectral density I of the unknown decohering environment.

C. The two Markovian limits of a damped harmonic oscillator

In order to put the findings of this work into context, we briefly discuss the two Markovian limits of the damped harmonic oscillator. Generally, the dynamics of a quantum system is Markovian if it is entirely forgetful [22–24]. Formally, this is usually grasped in the following way: Consider the map that maps the initial state of the system of interest (here the mechanical mode) to its state at a later time t , $\rho \mapsto T_t(\rho)$. T_t is a completely positive, trace-preserving map, called the dynamical map. One then says that the dynamics is Markovian, if $T_0 = \mathbb{I}$,

$$T_{t+s}(\rho) = (T_t \circ T_s)(\rho), \quad (49)$$

and a technical condition concerning continuity is satisfied. Then there exists a generator of the semi-group describing Markovian quantum dynamics. In essentially all physical situations this Markovian situation may typically be realised to an extraordinary extent or precision, in particular in the quantum optical context, but remains an approximation.

The damped harmonic oscillator has actually two different limits in which the dynamics becomes arbitrarily Markovian, an observation that is sometimes overlooked in the literature. Define the bath correlation time as

$$\tau_B = \max\{\Lambda^{-1}, \hbar/(2\pi k_B T)\}, \quad (50)$$

where Λ is the largest frequency present in the heat bath. Then one can distinguish the ‘quantum optical limit’ from the ‘quantum Brownian motion’ limit. The *quantum optical limit* is satisfied if

$$\tau_B \ll \gamma_\infty^{-1}, \quad \Omega_\infty^{-1} \ll \gamma_\infty^{-1}, \quad (51)$$

where γ_∞ is the effective damping constant and ω the free frequency. The *quantum Brownian motion limit*, in contrast, approximates the physical situation well if one has an Ohmic spectral density and

$$\tau_B \ll \gamma_\infty^{-1}, \quad \tau_B \ll \Omega_\infty^{-1}. \quad (52)$$

The quantum optical limit is, unsurprisingly, usually satisfied for quantum optical systems, where the damping is much smaller than the time scales of the free time evolution – in a situation where the so-called rotating wave approximation is valid to an extraordinary extent. In this regime, details of the spectral density also not matter at all, as merely the spectral density at the resonance contributes. This is not what we find in this work; as the Q -factor is with 215 relatively low, the spectral density also in the vicinity of resonance can be assessed. The quantum Brownian motion limit is more common in the condensed-matter context, where the bath correlation time is still short compared to all other time scales. This limit is associated with a high-temperature limit. This is closer to the situation discussed here.

D. Discussion of non-Markovian effects

The high temperature dynamics encountered here is non-Markovian for spectral densities other than Ohmic in the sense that Eq. (49) is violated. In technical terms, this also means that no time-independent generator of the dynamical map that takes Lindblad form can be found. For a detailed discussion of the influence of the spectral density on Markovianity properties of the open systems dynamics, see Ref. [21]. In general, the equations of motion of the mechanical oscillator are given by

$$\ddot{q}(t) + \Omega^2 q(t) + \frac{2}{m} \int_0^t ds \eta(t-s) q(s) = \frac{f(t)}{m}. \quad (53)$$

For an Ohmic spectral density,

$$I(\omega) = \gamma_\infty m \begin{cases} \omega, & \omega \in [0, \Lambda], \\ 0, & \text{otherwise,} \end{cases} \quad (54)$$

the damping kernel is for large cut-off frequencies Λ arbitrarily well approximated by

$$\eta(t) = \gamma_\infty m \delta'(t). \quad (55)$$

Note that for harmonic quantum systems, a time-local form of the equations of the reduced density operator can always exactly be achieved, for all spectral

densities. This is true for algebraic reasons, and not because the dynamics is Markovian. The memory inherent in the dynamics is then hidden in the intricate time dependence of the coefficients of the master equation.

However, the open systems dynamics is distinctly different in the case of a non-Ohmic spectral density:

- Firstly, the inhomogeneity of Eq. (7) explicitly depends on the spectral density and leads to properties different from what is expected in the Ohmic Markovian limit even for large times.
- For short times and in non-equilibrium, the dynamics is also in its nature very much altered, as is impressively discussed in Ref. [21]. This leads to a heavy time-dependence of the coefficients of the master equation, which are a consequence of memory-effects present in the system, reflecting the non-Markovian nature of the dynamics.

The spectral density responsible for this dynamics is estimated in the main text in the vicinity of the resonance.

E. Impact of technical noise

Several potential sources of technical noise in our experimental setup exist that could in principle influence the frequency dependence of the observed noise-floor and might have an impact on our experimental results. The emission from the laser itself, as well as the electro-optical modulator and the photo-detectors could introduce excess, frequency dependent noise, which however can easily be verified experimentally by measuring the light spectrum of the reflected laser field from an unlocked, far off-resonant optomechanical cavity. In the frequency band of interest, the noise floor is more than one order of magnitude below the thermal noise floor of the mechanical resonator and shows negligible frequency dependence, which is reflected in our experimental error bars. We further rule out noise from our optomechanical cavity, by measuring the same cavity without a mechanical element (see Fig. 2). This is done by moving to a mirror pad on the chip that is not released. In addition, electronic noise in our detection system plays a negligible role.

Finally, higher order mechanical modes could influence the frequency dependence of our measured noise floor. We have simulated our device and find that these modes do not influence the noise floor in the frequency window we are interested in any significant way. Note that any impact from higher order modes would make the coupling to the environment more supra-Ohmic rather than sub-Ohmic, as observed in our experiment.

F. Statistical analysis

In this section we describe the statistical analysis in more detail. We process raw data in the form of samples from a time series $\{\delta Y^{\text{out}}(t)\}$ obtained from the homodyne measurement with a 10 MHz sampling rate. From this, $m = 9,000$ batches are formed, each containing $n = 100,000$ data points. For every such batch, the data are Fourier transformed, to get data in the frequency domain, and the mean of 100 data sets is considered. In this way, 90 independently distributed spectra are obtained. For each of these 90 Fourier transforms, the optimal power k in Eq. (5) is being determined by fixing an interval $[\omega_{\min}, \omega_{\max}]$ around the renormalised resonance frequency Ω_∞ . For the present experiment, $\omega_{\min} = 885$ kHz and $\omega_{\max} = 945$ kHz have been chosen. As this minimisation task constitutes a non-convex optimisation problem, a global simulated annealing algorithm is used. Fig. 3 shows the outcome of this analysis. Again, while for each realisation of a spectrum several values of k are approximately compatible with the data, one can estimate the optimal k with high significance from the complete data set.

To further corroborate these findings, many variants of the above statistical estimation have been systematically explored. Notably, several instances of bootstrapping, involving a resampling of data, give rise to findings that are indistinguishable from the above ones. The results are largely independent against a different choice of the frequency window or the way batches are being chosen. Also, the findings are not different when not the least squares difference is being considered in the actual intensities, but the logarithms thereof.